Formation and Evolution of Single-Molecule Junctions

M. Kamenetska,[1,2] M. Koentopp,[2] A. C. Whalley,[3] Y. S. Park,[3] M. L. Steigerwald,[3,2]
C. Nuckolls,[3,2] M. S. Hybertsen,[4,*] and L. Venkataraman[1,†]

[1]*Department of Applied Physics and Applied Mathematics, Columbia University, New York, New York, USA*
[2]*Center for Electron Transport in Molecular Nanostructures, Columbia University, New York, New York, USA*
[3]*Department of Chemistry, Columbia University, New York, New York, USA*
[4]*Center for Functional Nanomaterials, Brookhaven National Laboratory, Upton, New York, USA*

(Received 22 December 2008; published 24 March 2009)

We analyze the formation and evolution statistics of single-molecule junctions bonded to gold electrodes using amine, methyl sulfide, and dimethyl phosphine link groups by measuring conductance as a function of junction elongation. For each link, the maximum elongation and formation probability increase with molecular length, strongly suggesting that processes other than just metal-molecule bond breakage play a key role in junction evolution under stress. Density functional theory calculations of adiabatic trajectories show sequences of atomic-scale changes in junction structure, including shifts in the attachment point, that account for the long conductance plateau lengths observed.

DOI: 10.1103/PhysRevLett.102.126803 PACS numbers: 73.63.Rt, 61.46.−w, 81.07.Nb, 85.65.+h

Over the past decade, the field of molecular scale electronics has come a long way towards elucidating and characterizing intrinsic molecular properties that affect transport. The electronic properties of single molecules attached to metal electrodes have been measured successfully by elongating and breaking nanometer scale wires in an environment of molecules using mechanically controlled break junctions and scanning tunneling microscopes (STMs) [1–4]. Typically, the focus of these measurements has been on conductance and current-voltage characteristics. The physical structure of a single, nanoscale junction, such as an Au point contact, however, has only rarely been directly observed [5]. As a result, the role of junction size, molecular conformation, and thermal fluctuations have been inferred from parametric measurements [6–9], but fundamental questions regarding link bond formation and junction evolution under stress remain to be answered.

Here we analyze a statistically significant sample of single-molecule junctions made by breaking Au point contacts in solution of the molecules using a simplified STM, recording junction conductance as a function of the relative tip-sample displacement [4]. These conductance versus displacement traces, measured with amine (NH_2), dimethyl phosphine (PMe_2), and methyl sulfide (SMe) links that bind selectively to gold [10], show plateaus during elongation, providing a signature of junction formation. The lengths of these plateaus for different molecules probe the amount of elongation a junction can sustain without breaking. We find that, across all end groups, longer molecules form longer conductance plateaus and have a higher probability of forming a junction. Changes in applied bias voltage or elongation speed have no discernible effect [11]. Density functional theory (DFT) based *ab initio* calculations simulating the junction elongation process for the NH_2 and PMe_2 links show clearly that the long steps result from multiple processes including changes in the molecular binding site, changes in the gold electrode structure, and molecular rearrangements, as well as bond breakage. Bond breakage contributes only a small fraction of the total junction elongation distance. Furthermore, the zero-bias transmission does not change significantly upon changes in the molecular binding site or gold electrode structure, consistent with the narrow peaks seen in the measured conductance histograms.

Individual conductance traces for 1,4-butanediamine (1), 1,6-hexanediamine (2), and 1,4-bis (dimethylphosphino) butane (3), measured under a bias of 25 mV with a pulling speed of 15 nm/s from a ~1 mM solution in 1,2,4 trichlorobenzene, are compared in the inset in Fig. 1(a). These traces show plateaus with molecule-dependent conductances and lengths; junctions of butane with the PMe_2 links (3) have the longest plateaus, sustaining the largest elongation, while those of butane with NH_2 links (1) have the smallest. Figure 1(a) shows the corresponding normalized conductance histograms generated from around 40 000 measured traces, without any data selection. The clear peak seen in these histograms reflects well the fact that molecular plateaus occur repeatedly within $\sim \pm 50\%$ (peak width) of a well-defined conductance value (peak position).

To distinguish differences in molecular plateau lengths, a two-dimensional (2D) histogram, retaining displacement information, is required [12,13]. Since conductance plateaus occur in random locations along the displacement axis, we first set the origin of the displacement axis at the point in the trace where the conductance drops below G_0. The 2D histograms, shown in Figs. 1(b)–1(d), are then created with linear bins along the positive displacement (x) axis and log bins along the conductance (y) axis for image clarity. [Note: Using log bins shifts the conductance peaks up by ~15% as shown in Fig. 1(e) [14]]. The

 © 2009 The American Physical Society

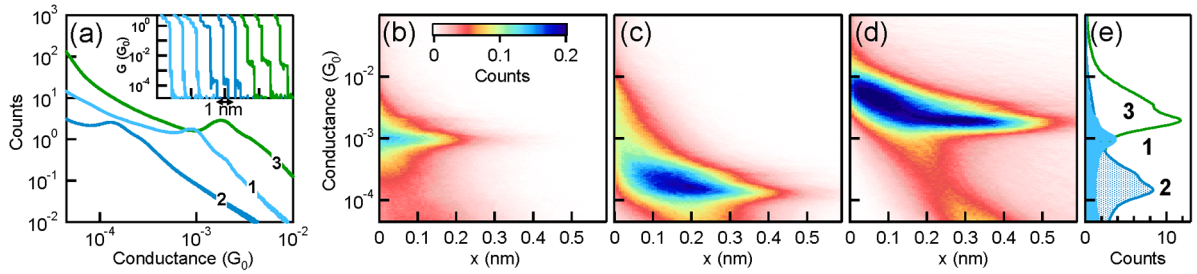

FIG. 1 (color online). (a) Normalized linear conductance histograms of 1,4-butanediamine (1, bin size $10^{-5}G_0$), 1,6-hexanediamine (2, bin size $10^{-6}G_0$), and 1,4-bis (dimethylphosphino) butane (3, bin size $10^{-5}G_0$). Inset: Sample conductance traces (offset horizontally for clarity) that show a molecular step for each molecule. (b)–(d) Normalized 2D histograms for molecules 1, 2, and 3, respectively (100 bin/decade against 0.007 nm/bin). (e) Normalized log-bin conductance histograms for 1, 2, and 3.

normalized 2D histograms show that the molecular conductance peak extends to approximately 2.5 Å along the x axis for 1, 4.5 Å for 2, and 5.5 Å for 3. Comparing the two diamines (1 and 2), we find more counts and longer plateaus for the longer molecule. We also see that PMe_2 links (3) sustain longer plateaus than NH_2 (1).

To quantify these trends, we determining the length of the molecular conductance plateau for each measured trace with an automated algorithm [15] for a series of alkanes with NH_2, SMe, and PMe_2 links. From a histogram of plateau lengths [Fig. 2(a)], we determine the "longest" plateau for each molecule measured, defined as the 95th percentile of the distribution [16]. In Fig. 2(b), we plot the longest step length as a function of the number of methylene (CH_2) groups on the alkane backbone. Comparing molecules with the same link group, we see a striking increase in junction elongation distance with molecule length. Linear fits to these data show a similar slope, but they are offset vertically, with the PMe_2 link having the largest intercept. This is consistent with our previous assertion that the elongation distance between the energy minimum configuration and the force maximum of a molecular junction increases from NH_2 to SMe to PMe_2 [10]. We also analyzed measurements of a series of oligophenyls (one, two, and three rings) with NH_2 links and find a similar linear increase in junction elongation with molecule length.

Our analysis shows that, in individual conductance traces, an Au point contact is thinned out to a single atom chain and breaks; then a molecular plateau is seen, with a length and frequency that depend on the molecule length. When the Au contact breaks, the Au atoms snap back [17] leaving two electrodes that are separated by about 6.5 ± 6.5 Å [12,17]. This suggests that, for junction formation, short molecules insert with the link groups bonded to the apex atom of the tip and substrate, while long molecules can bind away from one (or both) apex atoms. Once a junction is formed, upon elongation, the binding site could move from one atom to the next, or the gold electrodes could deform under the pulling force. This implies that longer molecules have access to a larger number of binding sites on the Au tip and substrate. Indeed, we find that the fraction of traces with steps increases systematically with molecule length from about 25% for ethanediamine to 65% for butanediamine, 85% for hexanediamine, and about 95% for octanediamine.

There are certainly alternative scenarios for junction formation. First, *gauche* defects in alkanes are relatively low energy, so a bent or folded conformation could bind at the apex [6] and unwind under tension resulting in longer conductance plateaus. However, in such cases, the junction conductance would initially be significantly lower, contrary to what we observe in the 2D histograms [8]. Also, such folding will not occur for oligophenyls. Second, molecules could already be bridging the tip and substrate in parallel to the Au point contact prior to gap formation [9]. While this would be very unlikely for the short molecules in our study, we cannot conclusively rule it out for longer molecules.

To probe molecular junction evolution, *ab initio* calculations of adiabatic pulling traces were conducted for 1 and 3 with different initial geometries. The contacts are modeled with Au pyramids (20 atoms each) with (111) surfaces. The tip atom on the top pyramid was moved to an adatom site on one facet. We considered starting geometries in which one link group was bound to an atom on the edge of the top pyramid (Fig. 3) or to the adatom on one of the faces (Fig. 4). We studied eight distinct junction structures, four with each link. These are illustrative scenarios that probe two types of Au link site (edge and adatom) and

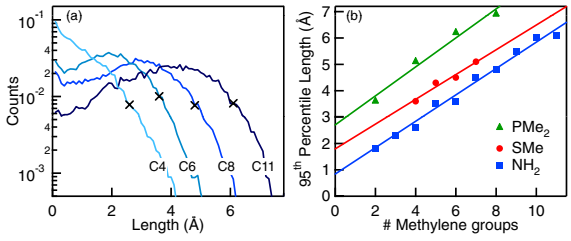

FIG. 2 (color online). (a) Conductance step length distribution for diamino alkanes with 4, 6, 8, and 11 CH_2 groups in the chain. Crosses indicate the 95th percentile for each distribution. (b) Conductance step length (95th percentile) as a function of the number of CH_2 groups for alkanes with the three links studied.

the influence of bond strength (amine versus phosphine). They include selected variations in molecular backbone angle and other constraints to probe the robustness of the main conclusions. The back layer of Au atoms for the top and the back two layers of the bottom pyramid were held fixed with a bulk lattice parameter 4.08 Å (except where noted below). All other degrees of freedom were relaxed until all forces were less than 0.005 eV/Å. The junction was then elongated in 0.05 Å steps by shifting the bottom pyramid along the z direction and then fully optimizing the geometry.

Total energy calculations and geometry optimization were performed with the quantum chemistry package TURBOMOLE v5.10 [18]. A DFT approach was used with a generalized gradient approximation functional (Perdew-Burke-Ernzerhof form) [19] and an optimized split valence basis set with polarization functions (designated def2-SVP) [20]. The ballistic electron transmission through the junction was calculated with a Green's function approach applied to the composite electrode-molecule system and a simplified embedding self-energy [21–23]. The zero-bias conductance is given by transmission at the Fermi energy. The Green's function was based on the eigenstates from the DFT calculation. Test conductance calculations for 1,4-benzenediamine agreed with earlier results [15]. While the DFT-derived frontier energy alignment results in systematic errors in the calculated conductance [15,24,25], errors are modest for alkanes as the Fermi energy is roughly in the middle of the gap between the highest occupied and lowest unoccupied molecular orbital energies [26].

Figure 3 shows an illustrative scenario where the NH_2 initially binds to the edge atom of the second layer of the upper pyramid [27]. The NH_2 remains coordinated to this Au atom for about 1.5 Å, with an increasing N-Au bond length. When it approaches a bridging geometry, the NH_2 abruptly jumps (at $z = 1.8$ Å) to bind to the lower, corner Au atom on the tip. Following the jump, the N-Au bond lengths remain relatively constant up to about $z = 3.5$ Å, with the geometry adjusting through bond angle changes. Then the bottom N-Au starts to elongate, and the maximum sustained force of 0.8 nN is observed near $z = 3.8$ Å. Up to $z = 3.8$ Å, the calculated conductance is consistent with a single step as it would be observed in the experiments. After $z = 3.8$ Å, the conductance decreases exponentially with N-Au bond elongation. The abrupt termination of experimental traces is consistent with energy cost to break the lower N-Au bond (<0.4 eV) at $z = 3.8$ Å and thermal fluctuations on the millisecond time scale. Calculations starting from a similar junction with PMe_2 links showed more extensive Au electrode deformations, including plastic deformation of the tip region and extraction of short Au chains. The P-Au bond to the lower pyramid broke after a 5–7 Å elongation with a maximum sustained force around 1.4 nN.

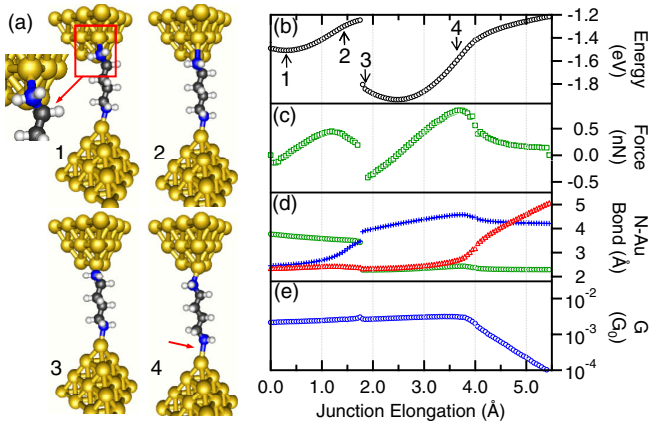

FIG. 3 (color online). Calculated adiabatic 1,4-butanediamine junction elongation trace. (a) Relaxed junction geometries at four different positions. (b) Binding energy relative to relaxed, isolated Au pyramids and molecule. (c) External applied force calculated from the derivative of junction energy with respect to elongation. (d) N-Au bond lengths: upper N to the Au atom on the second layer (+), to the Au atom on the bottom layer (□), and the lower N-Au bond (△). (e) Conductance.

Figure 4 shows a different scenario with a PMe_2 link initially bound to the Au adatom tip face [27]. There is an initial twist in the molecule (~0.2 eV energy cost) which could be realized in experiment due to constraints in available binding sites. The conductance thus starts low ($2–3 \times 10^{-4} G_0$) as the electronic gateway state of the P-Au link is not aligned with the sigma states of the alkane backbone. Under stress, the molecule untwists, initially slowly and then with a rapid readjustment at around $z = 3.3$ Å, and conductance rises to $\sim 4 \times 10^{-3} G_0$. At the same time, the Au adatom is dragged towards the edge of the pyramid, adopting a twofold coordination against the pyramid edge. At $z = 3.7$ Å, the nearest Au corner atom in the back layer is freed. This stabilizes the upper Au pyramid against significant plastic distortion. From $z = 3.9$ to 5.1 Å, the

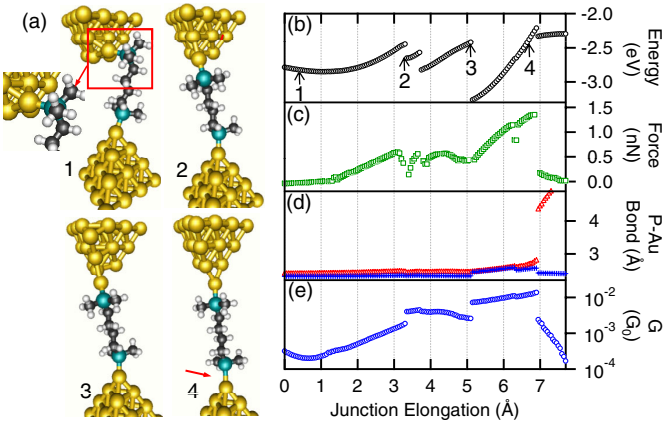

FIG. 4 (color online). Calculated adiabatic 1,4-bis(dimethylphosphino)-butane junction elongation trace. (a) Relaxed junction geometries at four different positions. (b) Binding energy. (c) External applied force. (d) P-Au bond length: upper (+) and lower (△) pyramids. (e) Conductance.

Au atoms around the adatom distort, and at $z = 5.1$ Å, the adatom abruptly jumps to the apex position with the conductance increasing to about $7 \times 10^{-3} G_0$. The P-Au bonds and Au apex structures stretch modestly with the lower P-Au bond taking up most of the elongation until it breaks at $z = 6.9$ Å. The conductance then decreases exponentially. The maximum sustained force is again about 1.4 nN, similar to the measured Au-Au breaking force [28]. Experimentally, such a trace would have an initial gap (low conductance value). Calculations done for similar junction structures with NH_2 links showed that the N-Au bond was strong enough only to pull the Au adatom up to a bridging position on the pyramid edge before the lower N-Au bond broke at a maximum sustained force of 0.8 nN.

An overview of all eight calculated trajectories shows that the junction formation energy at local minima spans the range 1.1–1.6 eV per PMe_2-Au bond (15 minima) and 0.7–1.0 eV per NH_2-Au bond (8 minima). With the exception of regions with a twist in the molecule, the calculated conductance values undergo modest changes when the link attachment point shifts or the Au atoms near the link rearrange. The calculated conductance values for 1 range from $1–3 \times 10^{-3} G_0$, while those for 3 span a broader range ($1–12 \times 10^{-3} G_0$). These are slightly larger than the experimental peak positions in Fig. 1(a) at approximately $1 \times 10^{-3} G_0$ (1) and $2 \times 10^{-3} G_0$ (3), though the ranges are consistent with the measured histogram widths. Finally, the twist in the molecule (*gauche* defect) results in a conductance smaller by 1 order of magnitude, in agreement with a very recent study of alkanedithiol junction evolution and conductance [29]. From the measured histograms, we conclude that such low conductance data are not statistically significant and could occur in less than 5% of the traces.

Several fundamental points emerge from our work. First, junctions can form with the link group bonded to an undercoordinated Au atom higher up on the electrode with similar binding energy and conductance. This naturally explains the higher probability of junction formation observed for longer molecules. Second, under stress, such junctions can evolve through different types of physical motion of the link, either by hopping of the link group from one available undercoordinated Au site to another (but never a bridge or hollow site) or by dragging an undercoordinated Au atom, thereby distorting the Au structure. During this motion, the conductance can be relatively stable, consistent with a single step in the measured traces. Third, the stronger Au-PMe_2 bond, compared with the Au-NH_2, can extend the physical junction over a larger distance, consistent with measurements. Finally, our results highlight the diversity of physical configurations that are probed when single-molecule junctions are formed. The consistent measured conductance signatures that form the well-defined steps derive from the chemical specificity of the donor-acceptor link motifs. The lone pair on the link atom (N from NH_2, S from SMe, and P from PMe_2) coordinates a single Au atom on the electrode. Thus local variations in electrode atomic structure and link geometry have only a modest influence on the electronic coupling.

We thank Ferdinand Evers for use of the advanced NEGF code. This work was supported in part by the NSEC program of the NSF (Grant No. CHE-0641532), NYSTAR, and a NSF Career grant (No. CHE-07-44185). Part of this research was performed at the CFN at BNL and supported by DOE (Contract No. DE-AC02-98CH10886). C. N. and L. V. thank the Columbia RISE grant for support.

*mhyberts@bnl.gov
†lv2117@columbia.edu

[1] M. A. Reed *et al.*, Science **278**, 252 (1997).
[2] J. Reichert *et al.*, Phys. Rev. Lett. **88**, 176804 (2002).
[3] B. Q. Xu and N. J. J. Tao, Science **301**, 1221 (2003).
[4] L. Venkataraman *et al.*, Nano Lett. **6**, 458 (2006).
[5] H. Ohnishi, Y. Kondo, and K. Takayanagi, Nature (London) **395**, 780 (1998).
[6] W. Haiss *et al.*, Nature Mater. **5**, 995 (2006).
[7] A. A. Kornyshev and A. M. Kuznetsov, Chem. Phys. **324**, 276 (2006).
[8] D. R. Jones and A. Troisi, J. Phys. Chem. C **111**, 14 567 (2007).
[9] E. H. Huisman *et al.*, Nano Lett. **8**, 3381 (2008).
[10] Y. S. Park *et al.*, J. Am. Chem. Soc. **129**, 15 768 (2007).
[11] Z. F. Huang *et al.*, Nature Nanotech. **2**, 698 (2007).
[12] S. Y. Quek *et al.*, Nature Nanotech. (to be published).
[13] C. A. Martin *et al.*, J. Am. Chem. Soc. **130**, 13 198 (2008).
[14] M. S. Hybertsen *et al.*, J. Phys. Condens. Matter **20**, 374115 (2008).
[15] S. Y. Quek *et al.*, Nano Lett. **7**, 3477 (2007).
[16] Although the 95th percentile is chosen arbitrarily, it gives a good measure of a statistically significant longest step, the geometrically relevant quantity probed here.
[17] A. I. Yanson *et al.*, Nature (London) **395**, 783 (1998).
[18] O. Treutler and R. Ahlrichs, J. Chem. Phys. **102**, 346 (1995); K. Eichkorn *et al.*, Chem. Phys. Lett. **240**, 283 (1995).
[19] J. P. Perdew, K Burke, and M Ernzerhof, Phys. Rev. Lett. **77**, 3865 (1996).
[20] F. Weigend, Phys. Chem. Chem. Phys. **8**, 1057 (2006); F. Weigend and R. Ahlrichs, Phys. Chem. Chem. Phys. **7**, 3297 (2005).
[21] F. Evers, F. Weigend, and M. Koentopp, Phys. Rev. B **69**, 235411 (2004).
[22] A. Arnold, F. Weigend, and F. Evers, J. Chem. Phys. **126**, 174101 (2007).
[23] With the 20 Au atom clusters, the self-energy ($\Gamma = 2.7$ eV) is applied to the back two planes. The calculated conductance is approximately constant for $\Gamma = 1–5$ eV.
[24] M. Koentopp, K. Burke, and F. Evers, Phys. Rev. B **73**, 121403(R) (2006).
[25] J. B. Neaton, M. S. Hybertsen, and S. G. Louie, Phys. Rev. Lett. **97**, 216405 (2006).
[26] Y. B. Hu *et al.*, Phys. Rev. Lett. **95**, 156803 (2005).
[27] An animated visualization of trajectories is available online at http://www.columbia.edu/~lv2117/Junctions08/.
[28] G. Rubio, N. Agrait, and S. Vieira, Phys. Rev. Lett. **76**, 2302 (1996).
[29] M. Paulsson *et al.*, Nano Lett. **9**, 117 (2009).